# Drop Printing of Pharmaceuticals: Effect of Molecular Weight on PEG Coated-Naproxen/PEG 3350 Solid Dispersions

**Hsin-Yun Hsu and Michael T. Harris**
Dept. of Chemical Engineering, Purdue University, West Lafayette, IN 47907

**Scott Toth and Garth J. Simpson**
Dept. of Chemistry, Purdue University, West Lafayette, IN 47907

*DOI 10.1002/aic.14979*
*Published online August 14, 2015 in Wiley Online Library (wileyonlinelibrary.com)*

*Solid dispersions have been used to enhance the bioavailability of poorly water-soluble active pharmaceutical ingredients (APIs). However, the solid-state phase, compositional uniformity, and scale-up problems are issues that need to be addressed. To allow for highly controllable products, the drop printing (DP) technique can provide precise dosages and predictable compositional uniformity of APIs in two-/three-dimensional structures. DP was used to prepare naproxen (NAP)/polyethylene glycol 3350 (PEG 3350) solid dispersions with PEG coatings of different molecular weights (MWs). A comparison of moisture-accelerated crystallization inhibition by different PEG coatings was assessed. Scanning electron microscopy, second harmonic generation microscopy, and differential scanning calorimetry analysis were performed to characterize the morphology and quantify the apparent crystallinity of NAP within the solid dispersions. Thermogravimetric analysis was employed to measure the water content within each sample. The results suggest that the moisture-accelerated crystallization inhibition capability of the PEG coatings increased with increasing MW of the PEG coating. Besides, to demonstrate the flexibility of DP technology on manufacturing formulation, multilayer tablets with different PEG serving as barrier layers were also constructed, and their dissolution behavior was examined. By applying DP and appropriate materials, it is possible to design various carrier devices used to control the release dynamics of the API.* © 2015 American Institute of Chemical Engineers *AIChE J*, 61: 4502–4508, 2015
*Keywords: drop printing, controlled release formulations, crystallization, drug release*

## Introduction

To increase dissolution rates and bioavailabilities of poorly water-soluble active pharmaceutical ingredients (APIs), solid dispersions have received extensive attention as a potential approach. Generally, a solid dispersion is composed of a hydrophobic API and a biologically inert polymer matrix. Solid dispersions can enhance the bioavailability of the API through mechanisms such as reduced API particle sizes, improved wettability, higher porosity, and the ability to reduce the crystallinity of the API. However, despite its advantages, solid dispersions are not prevalent in pharmaceuticals due to two main issues: physical and chemical instability, and the difficulty of processing and scaling up.[1–4]

To increase the stability of solid dispersions, moisture is one of the main factors that should be taken into consideration. In the presence of moisture, amorphous API and polymeric matrices could encounter moisture-induced phase separation in solid dispersions, decreasing the stability of the final product.[5,6] Additionally, the presence of moisture often accelerates the crystallization of compounds.[7,8] For poorly water-soluble APIs in solid dispersion, they are preferably produced into amorphous form as it has a higher energy than the crystalline counterpart and thus exhibits a higher dissolution rate and transient solubility.[9] Thus, crystallization of the product during storage is undesirable, and the higher the crystallinity the slower the dissolution rate. With an appropriately chosen coating, moisture can be prevented from coming into contact with the API, and the moisture-accelerated crystallization could be prevented.[10] It has been shown in food science that by using a proper coating, the shelf life of the food can be extended significantly.[11,12] The outer layer acts as a physical barrier, protecting materials inside from moisture, oxygen, and other physical and chemical entities that can cause degradation. The coating of samples is presumed to be beneficial to increasing the stability of the APIs, but currently studies are limited on the effect of moisture treatment on the coated final dosage formulations.[13]

Drop printing (DP) provides the ability to precisely and reliably distribute APIs within formulations. DP is a manufacturing technique, in which droplets are ejected one at a time with the application of an appropriate trigger. The solution being dispensed can be either solvent-based or a melt-based solution. DP can be applied to various dosage forms, and has the potential for developing individualized doses with controlled release, and the precision placement of drops can allow for the engineering of API release characteristics. Because of these merits, DP has been studied to evaluate its applicability in the

Correspondence concerning this article should be addressed to M. T. Harris at mtharris@purdue.edu.

pharmaceutical industry.[14–19] The majority of recent literature utilized the solvent-based system. Only limited results of the melt-based system have been presented.[20]

In this study, the feasibility to form drug delivery devices of solid dispersions by DP based on the melt system and the flexibility of DP to manufacture formulations was examined. This study was done in support of Test Bed 3, Drop Printing of API, in the Center for Structured Organic Particulates Engineering Research Center. In this Test Bed, API in molten solutions (melts) is printed on smooth, rough, or porous substrates, and in tablet forms. The solid dispersions are used to inhibit crystallization of the API; however, some of the melts have an affinity to moisture which promotes crystallization. This study will therefore investigate the effect of PEG coating layers on crystallization of the API in the solid dispersions.

Thus, two forms of samples were prepared in this study as the first phase of a multiphase effort to understand the effects of the coating layer and dosage form on the crystallization and dissolution dynamics of the API in the solid dispersions. First, a drop of the molten naproxen/polyethylene glycol 3350 (NAP/PEG 3350) solution was deposited on a glass slide. After 1 min, the solidified drop was covered by a layer of molten PEG that served as a barrier to moisture. PEG with different molecular weight (MW) was employed as the coating layer, and their ability to protect NAP from moisture was compared. The composite products were stored in 0% RH and 75% RH at room temperature. The interior solid dispersions were analyzed by scanning electron microscopy (SEM), second harmonic generation (SHG), and differential scanning calorimetry (DSC) to examine the effects of different covers on the crystallization of NAP with and without the presence of moisture. Thermogravimetric analysis (TGA) was employed to determine the water content in the samples. Second, DP was used to form multilayer tablets, and demonstrate its application on design of API carrier and release control. Different MWs of PEG served as the top and bottom layers of the multilayer tablets, and their influence on the releasing behavior of the API was compared. The goal of this study is to show the potential of applying DP on pharmaceutical manufacturing and its flexibility on designing drug-carrier devices with desired properties.

## Materials and Methods

### *Materials*

NAP was purchased from Spectrum Chemical (Gardena, CA). PEG (average MW 2000, 3350, 6000, and 8000) were purchased from Sigma–Aldrich (St. Louis, MO). Figure 1 shows the molecular structure of NAP and PEG. All other reagents and solvents were of analytical grade.

### *Sample preparation*

Two forms of samples were prepared as Figure 2 shows. For the first one, NAP and PEG 3350 were mixed with a ratio of 5:5 and melted in a syringe by a syringe heater to prepare a solid dispersion solution. A volume of 0.1 mL of the NAP/PEG 3350 solution was dispensed on a glass slide by a syringe pump. Right after solidification, the drops were covered with a 0.25 mL layer of PEG 2000, PEG 3000, PEG 6000, or PEG 8000. The samples were stored at room temperature in a 0% RH or 75% RH environment for 1 week. The saturated solution of sodium chloride was put inside a closed container to prepare 75% RH environment. The top layers were removed

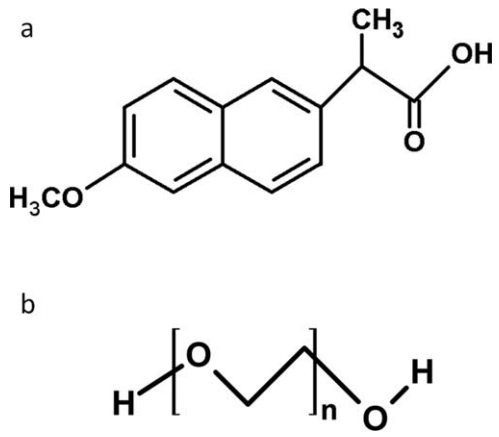


**Figure 1. Molecular structure of (a) naproxen and (b) polyethylene glycol.**

before analyzing the interior solid dispersions. This set of samples was examined by SEM, SHG, DSC, and TGA to characterize their morphology, apparent crystallinity, and water content.

To prepare multilayer tablets with different PEG serving as the barrier layers, molten solutions were dispensed into molds in the following order: 0.125 mL of PEG, then 0.2 mL of NAP/PEG 3350, finishing up with 0.125 mL PEG, where the top and bottom PEG layers were PEG 2000, PEG 3350, PEG 6000, or PEG 8000. Figure 2 shows the image of the multilayer tablet. These multilayer tablets were used to the study dissolution dynamics.

### *Scanning electron microscopy*

The morphology of solid dispersions on substrates was investigated by SEM (Model JSM-5600, JEOL Technics, Tokyo, Japan). Samples were cut in half and the cross-sectional area was gold sputter-coated to render them electrically conductive.

### *Second harmonic generation microscopy*

SHG microscopy was used to assess the extent of crystallinity within the prepared NAP/PEG samples. A custom-designed microscope was used with a Spectra-Physics Mai-Tai pulsed laser generating the incident light source with 800 nm pulses repeating at 80 MHz, with pulse widths of $\sim$150 fs, and an average of 30 mW at the sample. The laser was scanned across the sample with the use of an 8 kHz vibrating mirror (EOPC, Ridgewood, NY) on the fast-axis, and with a $\sim$100 Hz galvanometer-driven mirror (Cambridge Technologies, Lexington, MA) on the slow-axis. A 10x objective (Nikon, Melille, NY, 0.30 NA) was utilized to focus the light onto the sample, and the second harmonic at 400 nm was collected in the epi direction (i.e., back through the same objective in which the fundamental beam was introduced). The SHG signal was collected with a photo-multiplier tube (Hamamatsu R6094, Bridgewater, NJ), which was then digitized via a 12-bit PCI express digitizer (AlazarTech ATS9350, Pointe-Claire, QC, Canada). Software data acquisition was performed with MATLAB (MathWorks, Natick, MA) in addition to software and hardware designed by Purdue University's AMY Facility for Chemical Instrumentation. Further analysis was performed with ImageJ (NIH, Bethesda, MD).

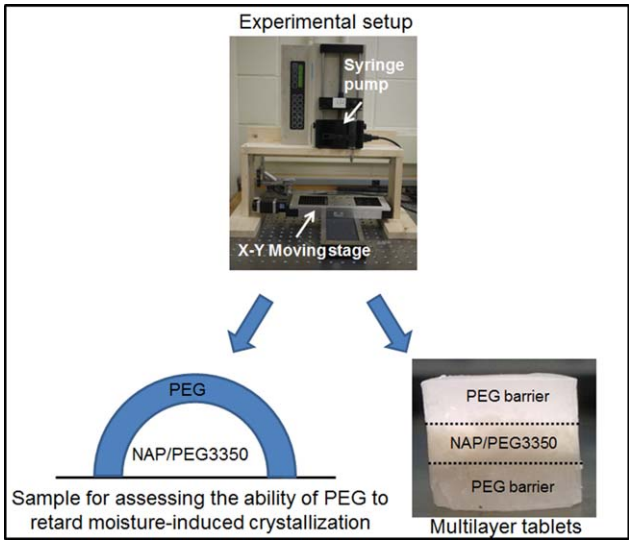


**Figure 2. Experimental setup and different forms of samples for this study.**

**[Color figure can be viewed in the online issue, which is available at wileyonlinelibrary.com.]**

### *Differential scanning calorimetry*

The apparent relative crystallinity of the solid dispersions beneath the various PEG coatings was determined with a differential scanning calorimeter Q2000 (TA Instruments, New Castle, DE). The instrument was calibrated for temperature using indium and tin and for enthalpy using indium. Dry nitrogen at 50 mL/min was used as the purge gas. Samples of 3–5 mg were analyzed using a heating rate of 20°C/min from 25 to 180°C. The relative crystallinity is evaluated as $x = \frac{\Delta H}{\Delta H_m}$, where $\Delta H$ is the melting enthalpy of crystalline NAP within the sample, and $\Delta H_m$ represents the melting enthalpy of 100% crystalline NAP at the same heating rate.[21] All experiments were done in triplicate.

### *Thermogravimetric analysis*

The water content within samples beneath PEG coating was estimated by TGA (TA instrument Q500). Ten milligram of the sample beneath PEG layer was taken, and heated from room temperature to 500°C with 20°C/min heating rate. The data were analyzed by the software TA Universal Analysis.

### *Dissolution testing*

The release dynamics of the multilayer tablets was analyzed with a dissolution test. Tablets were dissolved in 1 L of pH 7.4 phosphate buffer solution, within a jacketed flask (connected to a circulating water bath), utilizing a Corning stir plate for stirring. The temperature and stirring rate were 37°C and 100 rpm, respectively. At fixed time intervals, samples were withdrawn with a syringe filter (pore size 0.45 mm) and assayed by a Cary 100 UV-Vis spectrometer (Varian, Palo Alto, CA) for drug content. All experiments were performed in triplicate.

## Results

### *Scanning electron microscopy*

The morphology of the samples was examined by SEM. Figure 3 shows cross-sectional images of NAP/PEG 3350 solid dispersions with different PEG coatings. The samples were stored at 0% RH or 75% RH. Figures 3a–d are samples stored at 0% RH. Regardless of the MW of coatings, the topology of each sample stored at 0% RH was similarly smooth, whereas samples stored at 75% RH had a relatively rougher surface compared with those stored at 0% RH (Figures 3e–h). As the MW of the PEG coating increased, the morphology became smoother. An image of the sample covered by PEG 8000 (Figure 3h) appeared similar to samples stored at 0% RH. The morphological similarity between samples stored at 0% RH suggests the difference between samples at 75% RH was caused by moisture.

### *Second harmonic generation*

The apparent crystallinity of each sample was quantified via SHG. It is a useful tool for the examination of crystalline samples, allowing for high signal-to-noise measurements, with low limits of detection.[22–24] SHG involves the frequency-doubling of light upon interaction with certain classes of non-centrosymmetric crystals.[23] It has recently been applied to quantify crystallinity without the need for any additional sample processing.[22,25]

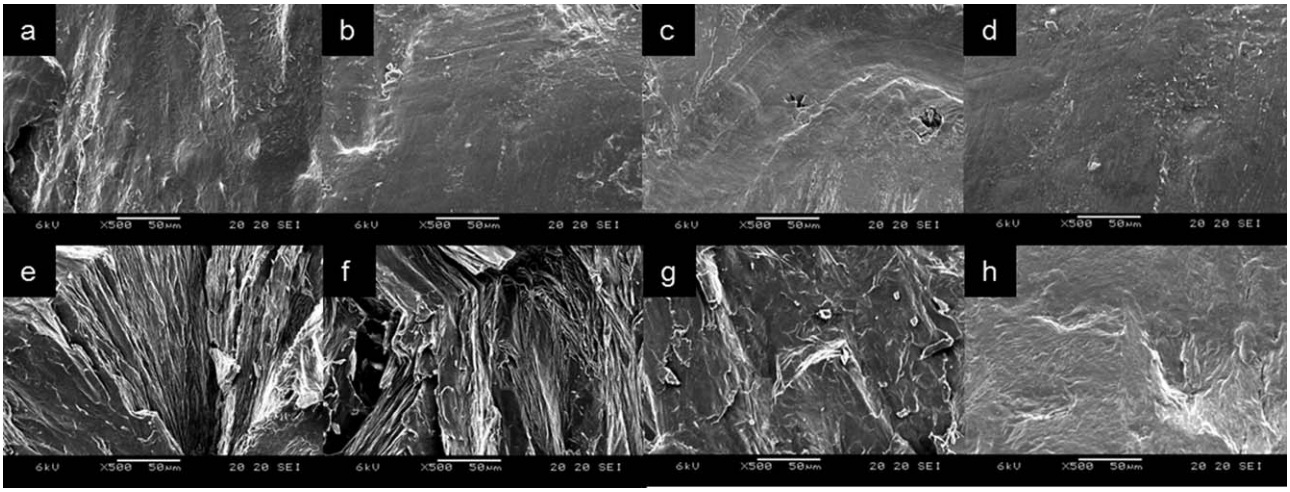


**Figure 3. SEM images of samples stored at (a) 0% RH PEG 2000 covered, (b) 0% RH PEG 3350 covered, (c) 0% RH PEG 6000 covered, (d) 0% RH PEG 8000 covered, (e) 75% RH PEG 2000 covered, (f) 75% RH PEG 3350 covered, (g) 75% RH PEG 6000 covered, and (h) 75% RH PEG 8000 covered.**

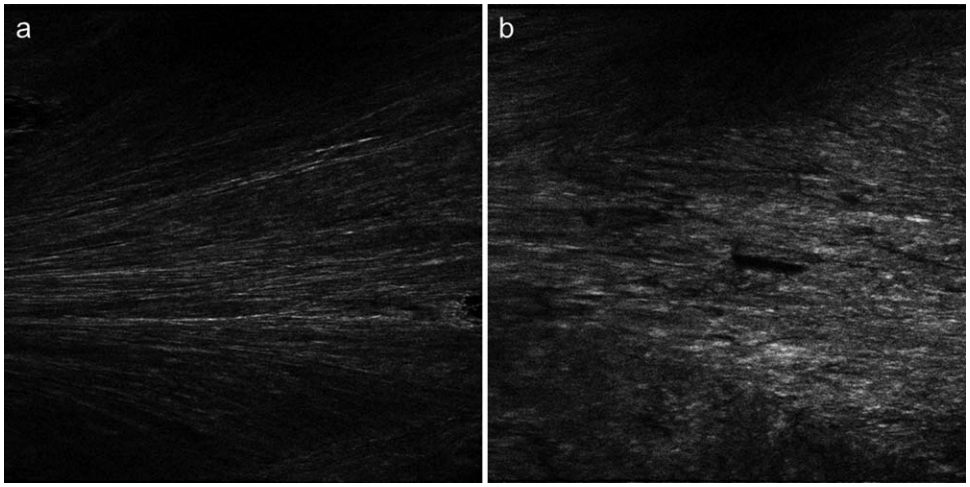


**Figure 4. SHG image of NAP/PEG 3350 covered by (a) PEG 8000 and (b) PEG 2000, stored at 75% RH.**

Figure 4 includes representative SHG images of the samples covered by PEG 2000 as well as samples covered by PEG 8000 stored at 75% RH. Both samples are displayed under the same brightness and contrast settings. The PEG 2000 covered sample appears brighter compared with the sample covered by the PEG 8000 layer, suggesting NAP crystallized to a greater extent within the uncovered sample. The average intensity of SHG image of each sample was normalized by the value of the sample stored at 75% RH without PEG cover and used to quantify the apparent crystallinity. The result is shown in Figure 5, in which the average SHG intensity is proportional to the volume of crystalline NAP. When stored at 0% RH, the MW of the PEG coating did not affect the apparent crystallinity, and each sample had a similar value in the range from 0.2 to 0.5.Whereas values of samples stored at 75% RH exhibited a trend that correlated with the MW of the PEG coatings. The PEG 8000-coated sample produced the lowest SHG intensity, and as the MW of the coatings decreased, the relative crystallinity increased while the samples covered by PEG 6000 and PEG 8000 had similar values. The data were also analyzed by *t*-test. It shows the sample covered by PEG 2000 did not have significant difference compared with sample without coating. For samples covered by PEG 3350, 6000, and 8000, the coated samples did show significant difference compared with the sample without coverage, indicating PEG layer with higher MW can slow down the crystallization.

### *Differential scanning calorimetry*

The difference in apparent crystallinity between samples was also confirmed by DSC. DSC has been widely used to quantify apparent crystallinity.[21,26] It has a lower limit of detection, and analysis requires a smaller quantity of materials in comparison to x-ray powder diffraction.[27] DSC was utilized to quantify the extent of crystallization of NAP within the NAP/PEG 3350 solid dispersion under different coatings.

Figure 6 exhibits DSC curves of PEG 2000-covered (6a) and pure NAP (6b) samples. Curve 6b displays the melting of pure NAP with a melting point at 154°C. Curve 6a shows two endothermic peaks. The first peak at 54°C indicates the melting of PEG 3350, and the second peak at 141°C corresponds to the melting of crystalline NAP within the sample. A melting point depression of NAP within the NAP/PEG solid dispersion sample was observed. Thermodynamically, the changes in the melting behavior of NAP arose because as the polymer

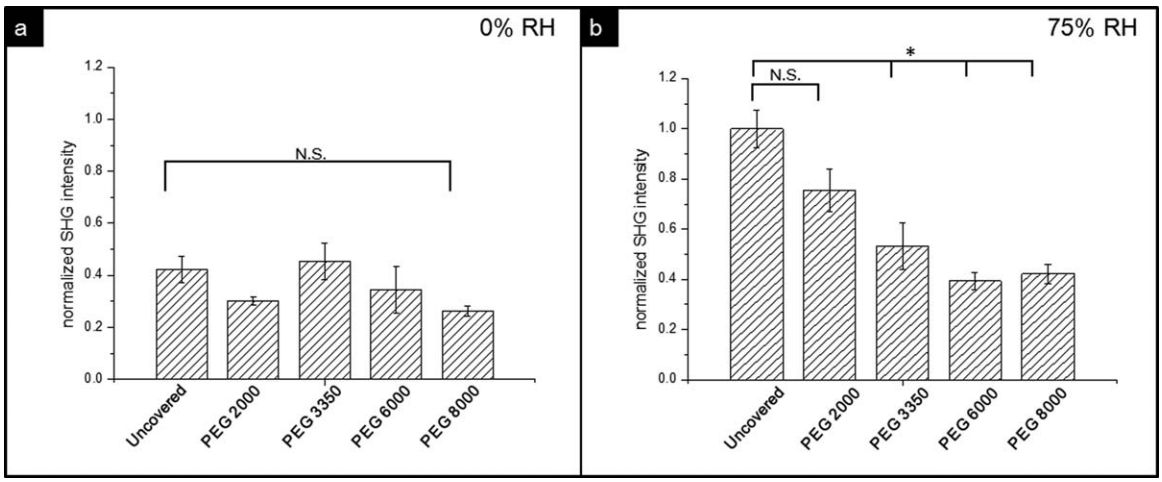


**Figure 5. Apparent crystallinity of NAP/PEG 3350 with coverage of different PEG that stored at 0% RH and 75% RH assessed by SHG microscopy. *Statistical significance at a level of $P < 0.05$; N.S., not significant.**

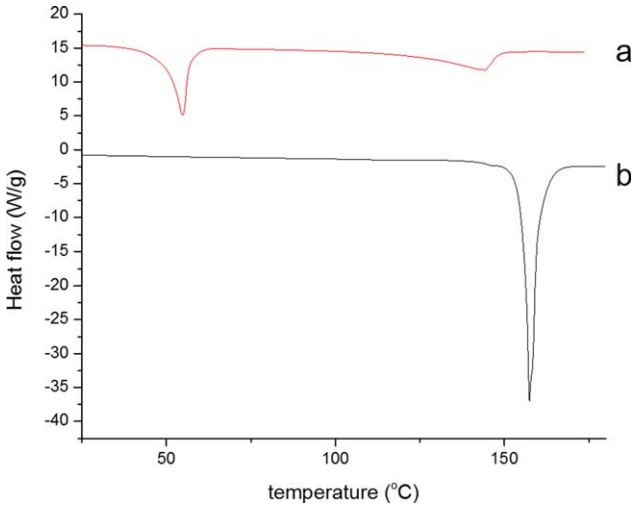


**Figure 6. DSC curve of (a) PEG 2000 covered NAP/PEG 3350 sample and (b) pure NAP.**

**[Color figure can be viewed in the online issue, which is available at wileyonlinelibrary.com.]**

spontaneously mixes with the liquid phase of the drug there is a negative free energy of mixing which lowers the chemical potential of the drug in the mixture relative to the pure liquid drug. This makes the melting process more thermodynamically favored, leading to melting point depression. Conceptually, melting point depression of APIs within a polymer matrix is similar to dissolution of the drug into the polymer.[28] The area under the second peak of each solid dispersion sample was integrated and divided by the area of the endothermic peak of curve 6b to quantify the apparent crystallinity of NAP within each sample.

Figure 7 shows that samples stored at 0% RH had a similar extent of crystallization and the value is less than any sample stored at 75% RH. Whereas, for samples stored at 75% RH, the apparent crystallinity increased when the MW of the coatings decreased. Interestingly, samples covered by PEG 6000 resulted in crystallinity similar to those of samples covered by PEG 8000. Similar to the results of SHG, after stored at 75% RH, there is significant difference between samples without cover and those covered by higher MW PEG.

### *Thermogravimetric analysis*

The water content within NAP/PEG 3350 under different PEG layers was estimated by TGA. Figure 8 shows the TGA curve of the NAP/PEG 3350 beneath the PEG 2000 layer. The curve demonstrates three steps of weight loss. The first one before 200°C corresponded to water loss, the second one between 200 and 360°C related to decomposition of NAP, and the third step between 360 and 500°C was caused by decomposition of PEG 3350. No water loss was observed within samples stored at 0% RH (data not shown), and the water content within each sample stored at 75% RH was summarized in Table 1. The weight percent corresponded to water loss decreased with increasing MW of the PEG layer indicates high MW PEG layer has higher ability to inhibit water to penetrate and diffuse in the sample.

### *Dissolution tests*

To demonstrate the flexibility of the DP system on manufacture formulations and dictate the releasing of the API, multilayer tablets were formed, and their releasing behavior was compared with plain tablets.

PEG with different MW was used to be the top and bottom layers of the multilayer tablets. The dissolution curves for these samples are provided in Figure 9. The enhanced release rate observed at the beginning for a short time of the release process is known as burst effect and is many times undesirable as it may have negative therapeutic consequences (e.g., toxicity due to increase of the concentration of the API beyond the acceptable higher limits). The burst effect was obvious for tablets without layering and tablets with PEG 2000 and 3350 as the barrier layers. One hundred percent of the NAP within those tablets was released within 15 min. The samples coated by various PEG showed a decrease in the dissolution rate with an increase in the MW of the PEG layers. NAP within the tablets which had PEG 8000 as the barrier layers exhibited a much slower releasing behavior and it took 20 min longer for NAP to be fully released in comparison to those layered by low MW PEG.

## Discussion

The physical and chemical stability of APIs in formulations is generally affected by moisture. The plasticizing effect of

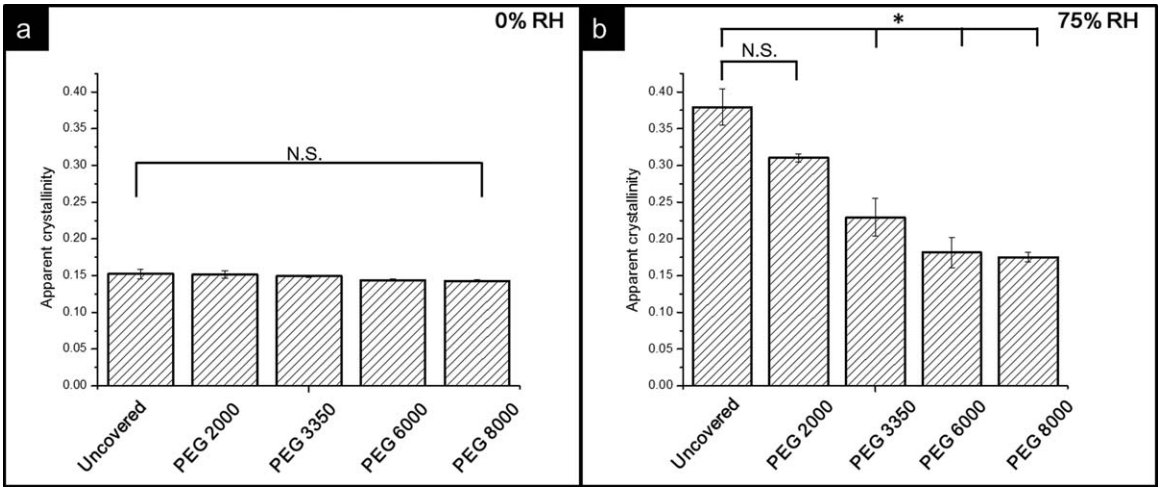


**Figure 7. Relative crystallinity of NAP/PEG 3350 with and without different coverage that stored at 0% RH and 75% RH assessed by DSC. *Statistical significance at a level of $P < 0.05$; N.S., not significant.**

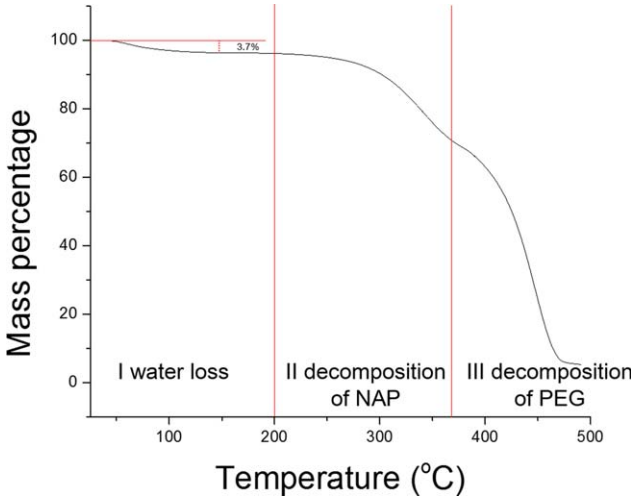


**Figure 8. TGA curve of NAP/PEG 3350 covered by PEG 2000 stored at 75% RH.**

**[Color figure can be viewed in the online issue, which is available at wileyonlinelibrary.com.]**

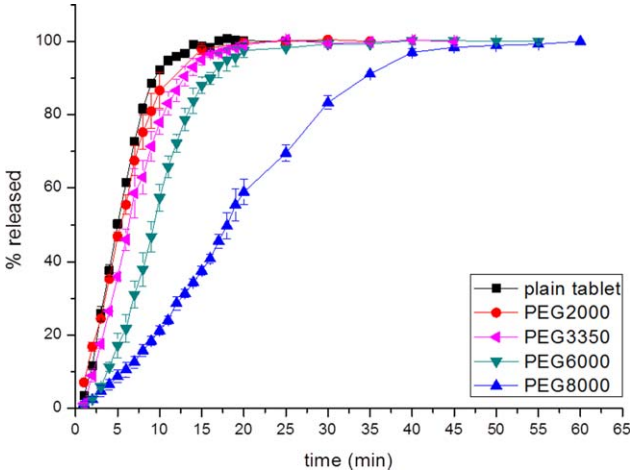


**Figure 9. Dissolution curves of NAP from plain tablet and multilayer tablets that composed by different PEGs as the top and bottom layers.**

**[Color figure can be viewed in the online issue, which is available at wileyonlinelibrary.com.]**

moisture on many systems has been found and widely accepted.[29]

To prevent moisture-induced instability, packaging is often utilized. The exterior coating of pharmaceutical final dosage forms can exclude moisture from coming into contact with the API. Therefore, selecting an appropriate material for the coatings is very important. The ability of PEG with different MWs to protect NAP, an API, from moisture-accelerated crystallization was compared. Samples stored at 0% RH were the control group to confirm the difference in the degree of crystallization with samples stored at 75% RH was because of different capability of PEGs to avoid moisture penetration. From the SEM, SHG, and DSC results, we found that samples stored at 0% RH crystallized to a lesser extent than samples that were stored at 75% RH, and had a smooth morphology. There was also no evident difference between the samples stored at 0% RH, whereas samples that were stored at 75% RH exhibited a decrease in NAP crystallinity with an increase in MW of the PEG.

PEG's ability to absorb water is mainly governed by the presence of ether oxygen atoms (—O—) in the oxyethylene polymer backbone as well as hydroxyl (—OH) end groups (Figure 1), both of which can form numerous hydrogen bonds with water.[30–32] PEG with different MWs have different polymeric chain lengths, which affects the aqueous solubility. As the MW of PEG increases, the relative fraction of hydroxyl endgroups decreases, and the higher MW grades are less hydrophilic and will have a lower aqueous solubility. Thermodynamically, as the chain length increases, the entropy of mixing of the polymer with water will be reduced which will also contribute to a decreased aqueous solubility.[33] Therefore, PEG's capability for water absorption increases with decreasing MW. The absorbed water increases the mobility of API within the samples and promotes crystallization. In our experiments, the impact of moisture reached an asymptote once the MW of PEG coating had increased to 6000. The apparent crystallinity of NAP covered by PEG 6000 was similar to the samples covered by PEG 8000.

**Table 1. Water Content with NAP/PEG 3350 Stored at 75% RH**

| Sample | Weight Percent of Water Loss (%) |
|---|---|
| NAP/PEG 3350 covered by PEG 2000 | 3.7 |
| NAP/PEG 3350 covered by PEG 3350 | 1.6 |
| NAP/PEG 3350 covered by PEG 6000 | 0.4 |
| NAP/PEG 3350 covered by PEG 8000 | 0.1 |

Besides, when building multilayer tablets, the different MW of PEG has an influence on the releasing rate of NAP. The multilayer tablets are often prepared to modify the release of APIs by controlling its diffusion within the matrix. Generally, the axial and radial mass transport of the API occurs during dissolution of the tablets. For multilayer tablets, the surface area of the core layer which contains the API was restricted by the addition of barrier layers to the both sides of the tablet, so the axial diffusion is retarded. In our experiments, PEG was used as the top and bottom barrier layers. When the barrier layers dissolve, the area of the active core exposed to the dissolving medium increases. Depending on the swell/dissolution rate of the barrier layers, hydration and the releasing rate of the active solute at the core changes. The three-layer tablets made with low MW PEG dissolved similarly as tablets without any layering. The burst effect was obvious and NAP released fast. As the MW increases, the aqueous solubility of PEG decreases. Hence, the barrier layers consist of PEG 8000 swollen and eroded much slower than the others, resulting in NAP in the active core releasing more slowly. The axial diffusion was delayed by the longer passage, so the releasing rate was retarded. By utilizing the DP technique, packaging formulations have been varied, providing additional degrees of freedom to the design of multilayer tablets. By selecting the proper materials, modulating layers, and changing the geometry of the drug delivery device, various dissolution patterns, such as delayed, pulsatile, or multimodal delivery profiles, can also be achieved.[33]

The ability of PEG layer to retard moisture-accelerated crystallization in the solid state is related to deliquesce of the layer. From a previous study, the effect of MW on critical relative humidity ($RH_0$) of PEG is a maximum at 6000. Therefore, the NAP/PEG stored at 75% RH had similar crystallinity when coated with PEG 6000 and 8000. Whereas, when we

used PEG with different MWs to control the releasing of NAP, there was clear difference in dissolution rate between tablets constructed with PEG 6000 and PEG 8000. These results indicated MW had influence on the aqueous solubility of PEG at MW between 6000 and 8000, but its impact on deliquesce of crystalline PEG had achieved the highest extent when MW gets 6000.

## Conclusions

The DP technique was utilized with a melted dispensing solution in this study. The ability of PEG, with different MWs, acted as a coating to protect NAP/PEG 3350 solid dispersions from moisture-accelerated crystallization. The results suggested that the ability of the coatings to prevent water from entering the interior of the samples increased with increasing MW of the PEG coatings. By applying DP and appropriate coating materials, the design of drug-carrying devices can be very diverse, and can lead to various releasing characteristics that are required of the API delivery.

## Acknowledgments

The authors would like to acknowledge the financial support from the National Science Foundation Engineering Research Center for Structured Organic Particulate Systems. SJT and GJS gratefully acknowledge additional support from NIH-R01GM103401. The authors declare no personal financial interests.

## Literature Cited

1. Dhirendra K, Lewis S, Udupa N, Atin K. Solid dispersions: a review. *Pak J Pharm Sci*. 2009;22(2):234.
2. Janssens S, Van den Mooter G. Review: physical chemistry of solid dispersions. *J Pharm Pharmacol*. 2009;61(12):1571–1586.
3. Serajuddin A. Solid dispersion of poorly water-soluble drugs: early promises, subsequent problems, and recent breakthroughs. *J Pharm Sci*. 1999;88(10):1058–1066.
4. Vasconcelos T, Sarmento B, Costa P. Solid dispersions as strategy to improve oral bioavailability of poor water soluble drugs. *Drug Discov Today*. 2007;12(23):1068–1075.
5. Rumondor AC, Marsac PJ, Stanford LA, Taylor LS. Phase behavior of poly (vinylpyrrolidone) containing amorphous solid dispersions in the presence of moisture. *Mol Pharm*. 2009;6(5):1492–1505.
6. Rumondor AC, Taylor LS. Effect of polymer hygroscopicity on the phase behavior of amorphous solid dispersions in the presence of moisture. *Mol Pharm*. 2010;7(2):477–490.
7. Shamblin SL, Zografi G. The effects of absorbed water on the properties of amorphous mixtures containing sucrose. *Pharm Res*. 1999; 16(7):1119–1124.
8. Andronis V, Yoshioka M, Zografi G. Effects of sorbed water on the crystallization of indomethacin from the amorphous state. *J Pharm Sci*. 1997;86(3):346–351.
9. Hancock BC, Zografi G. Characteristics and significance of the amorphous state in pharmaceutical systems. *J Pharm Sci*. 1997; 86(1):1–12.
10. Waterman KC, MacDonald BC. Package selection for moisture protection for solid, oral drug products. *J Pharm Sci*. 2010;99(11): 4437–4452.
11. Bourlieu C, Guillard V, Vallès-Pamiès B, Guilbert S, Gontard N. Edible moisture barriers: how to assess of their potential and limits in food products shelf-life extension? *Crit Rev Food Sci Nutr*. 2009; 49(5):474–499.
12. Greener I, Fennema O. Evaluation of edible, bilayer films for use as moisture barriers for food. *J Food Sci*. 1989;54(6):1400–1406.
13. Nikowitz K, Pintye-Hódi K, Regdon G Jr. Study of the recrystallization in coated pellets – effect of coating on API crystallinity. *Eur J Pharm Sci*. 2013;48:563–571.
14. Yeo Y, Basaran OA, Park K. A new process for making reservoir-type microcapsules using ink-jet technology and interfacial phase separation. *J Control Release*. 2003;93(2):161–173.
15. Scoutaris N, Hook AL, Gellert PR, Roberts CJ, Alexander MR, Scurr DJ. ToF-SIMS analysis of chemical heterogenities in inkjet micro-array printed drug/polymer formulations. *J Mater Sci Mater Med*. 2012;23(2):385–391.
16. Sandler N, Määttänen A, Ihalainen P, Kronberg L, Meierjohann A, Viitala T, Peltonen J. Inkjet printing of drug substances and use of porous substrates-towards individualized dosing. *J Pharm Sci*. 2011; 100(8):3386–3395.
17. Meléndez PA, Kane KM, Ashvar CS, Albrecht M, Smith PA. Thermal inkjet application in the preparation of oral dosage forms: dispensing of prednisolone solutions and polymorphic characterization by solid-state spectroscopic techniques. *J Pharm Sci*. 2008;97(7): 2619–2636.
18. Genina N, Fors D, Vakili H, Ihalainen P, Pohjala L, Ehlers H, Kassamakov I, Haeggström E, Vuorela P, Peltonen J. Tailoring controlled-release oral dosage forms by combining inkjet and flexographic printing techniques. *Eur J Pharm Sci*. 2012;47:615–623.
19. Hsu HY, Toth SJ, Simpson GJ, Taylor LS, Harris MT. Effect of substrates on naproxen-polyvinylpyrrolidone solid dispersions formed via the drop printing technique. *J Pharm Sci*. 2013;102(2):638–648.
20. Bashiri-Shahroodi A, Nassab PR, Szabó-Révész P, Rajkó R. Preparation of a solid dispersion by a dropping methodto improve the rate of dissolution of meloxicam. *Drug Dev Ind Pharm*. 2008;34(7):781–788.
21. Yang J, Grey K, Doney J. An improved kinetics approach to describe the physical stability of amorphous solid dispersions. *Int J Pharm*. 2010;384(1):24–31.
22. Wanapun D, Kestur US, Kissick DJ, Simpson GJ, Taylor LS. Selective detection and quantitation of organic molecule crystallization by second harmonic generation microscopy. *Anal Chem*. 2010;82(13): 5425–5432.
23. Kissick DJ, Wanapun D, Simpson GJ. Second-order nonlinear optical imaging of chiral crystals. *Annu Rev Anal Chem*. 2011;4:419–437.
24. Wanapun D, Kestur US, Taylor LS, Simpson GJ. Single particle nonlinear optical imaging of trace crystallinity in an organic powder. *Anal Chem*. 2011;83(12):4745–4751.
25. Kestur US, Wanapun D, Toth SJ, Wegiel LA, Simpson GJ, Taylor LS. Nonlinear optical imaging for sensitive detection of crystals in bulk amorphous powders. *J Pharm Sci*. 2012;101(11):4201–4213.
26. Lappalainen M, Pitkänen I. Quantification of amorphous content in maltitol by StepScan DSC. *J Therm Anal Calorim*. 2006;84(2):345–353.
27. Nagapudi K, Jona J. Amorphous active pharmaceutical ingredients in preclinical studies: preparation, characterization, and formulation. *Curr Bioact Compd*. 2008;4(4):213–224.
28. Baird JA, Taylor LS. Evaluation of amorphous solid dispersion properties using thermal analysis techniques. *Adv Drug Deliv Rev*. 2012; 64(5):396–421.
29. Hancock BC, Zografi G. The relationship between the glass transition temperature and the water content of amorphous pharmaceutical solids. *Pharm Res*. 1994;11(4):471–477.
30. Schachter DM, Xiong J, Tirol GC. Solid state NMR perspective of drug–polymer solid solutions: a model system based on poly (ethylene oxide). *Int J Pharm*. 2004;281(1):89–101.
31. Thijs HM, Becer CR, Guerrero-Sanchez C, Fournier D, Hoogenboom R, Schubert US. Water uptake of hydrophilic polymers determined by a thermal gravimetric analyzer with a controlled humidity chamber. *J Mater Chem*. 2007;17(46):4864–4871.
32. Kjellander R, Florin E. Water structure and changes in thermal stability of the system poly (ethylene oxide)–water. *J Chem Soc Faraday Trans 1*. 1981;77(9):2053–2077.
33. Baird JA, Olayo-Valles R, Rinaldi C, Taylor LS. Effect of molecular weight, temperature, and additives on the moisture sorption properties of polyethylene glycol. *J Pharm Sci*. 2010;99(1):154–168.

*Manuscript received Mar. 6, 2014, and revision received Oct. 5, 2014.*